The Eurasia Proceedings of Science, Technology, Engineering & Mathematics (EPSTEM)
ISSN: 2602-3199

The Eurasia Proceedings of Science, Technology, Engineering & Mathematics (EPSTEM), 2024

Volume 32, Pages 106-115

IConTES 2024: International Conference on Technology, Engineering and Science

Micro-Jet Control of Flow in NACA 4412 Wing

Hocine Tebbiche
Mouloud Mammeri University of Tizi-Ouzou

Mohammed Saîd Boutoudj
Mouloud Mammeri University of Tizi-Ouzou

Abstract: The separation and coherent structures resulting from the fluid detachment and the presence of marginal wing vortices lead to a decline in aerodynamic performance, noise generation, and vibrations. To address these issues, boundary layer control through blowing via micro-jets proves to be a highly effective solution, as it allows for a significant input of momentum near the wall. An experimental study, based on continuous tangential blowing through a series of micro-orifices, was conducted in a wind tunnel to analyze the effect on the flow over the upper surface of a NACA 4412 wing. Force measurements were taken for various velocities and angles of incidence. Wall and wake pressure measurements also carried out. The results obtained indicate that the blowing effect depends on the location of the blowing orifices and the ejected air flow rate. The analysis of drag and pressure mappings in the wake reveals that blowing near the wingtip generally leads to the generation of a more intense trailing vortex, causing the production of parasitic drag. Furthermore, lift results show a maximum relative gain of 37% at a Reynolds number of 1.6×10^5, accompanied by a 2-degree delay in stall.

Keywords: NACA 4412 wing, Boundary layer, Drag and lift, Pressure coefficient, Blowing

Introduction

In the flow around a wing, the separation of the boundary layer (Schlichting et al., 1979), and the presence of tip vortices result in energy dissipation and the generation of vibrations and noise. Boundary layer control techniques (Gad-el-Hak, 2001). Make it possible to decrease, or even eliminate, the separated region, thus reducing energy consumption and, consequently, lowering greenhouse gas emissions.

Solutions for control have been proposed in previous studies to reduce drag (Manolesos et al., 2015) increase lift (Satar et al., 2024) and mitigate the wake vortex area (Haverkamp et al., 2005). The winglet-wing configuration is the simplest among non-planar wings. Other suggestions include box wings or closed wings (Kroo, 2001). However, all non-planar wings suffer from structural complexity and increased weight (Jupp, 2001). Various leading-edge devices have also been considered for noise reduction (Slooff, 2002). And alleviating the wake vortex issue (Coustols et al., 2003)

The main drawback of most of the aforementioned leading-edge devices is that they are fixed on the wing and can only be optimized for a single flight condition, thus being less effective during the rest of the flight. In contrast, the use of an active means of flow control ensures optimal aircraft performance across the entire flight envelope. Active control can be implemented using movable parts, such as flaps, but this could lead to structural issues. That's why a number of researchers have focused on the blowing strategy. Numerous experimental studies are currently dedicated to investigating this control strategy (Bourgois, 2006; Roumeas, 2006; Chen et al., 2024). Favier et al., 2005 conducted a study on controlling the onset of separation on the upper surface of an ONERA D-type airfoil using blowing through a series of micro-jets inclined at 90° to the chord. A slight

increase in lift is recorded with this configuration; which leaves us with fairly broad paths of exploration in order to define new trends in optimization.

In this paper, we present an experimental study aimed at improving the aerodynamic characteristics of a NACA 4412 wing with a 5° sweep angle, a mid-chord length of 140 mm, and a span of 200 mm. The active control strategy employed in this study is continuous blowing through micro-jets. Micro-holes with a diameter of 0.6 mm are linearly arranged on the wing upper surface, at 10% from the leading edge. Unlike conventional control strategies, blowing through the micro-jets allows for a much deeper penetration of the jet into the flow and results in air consumption savings.

The experimental study is divided into two main components. The first part focuses on the wind tunnel investigation of the airfoil and the NACA 4412 wing's behavior concerning separation, assessed through the measurement of aerodynamic forces and uncontrolled flow pressure measurements. The second part addresses the effect of varying the blowing rate, wing angles of attack, and the upstream free-stream velocity, while keeping a focus on the control efficiency regarding the aerodynamic stall phenomenon.

Experimental Device

Wind Tunnel and Acquisition Chain

All experiments were conducted in a Deltalab™ type wind tunnel. The maximum measurable velocity exceeds 40 m/s. The turbulence level is set by a grid at the inlet with a size of 5×5 mm^2. The test section length and cross-sectional area are 100 cm and 30×30 cm^2, respectively (Figure 1). Lift and drag forces were measured using an aerodynamic balance connected to a data acquisition system. Each conducted test was repeated three times, and the average was considered. The acquisition time was set to 60 s with a frequency of 500 Hz.

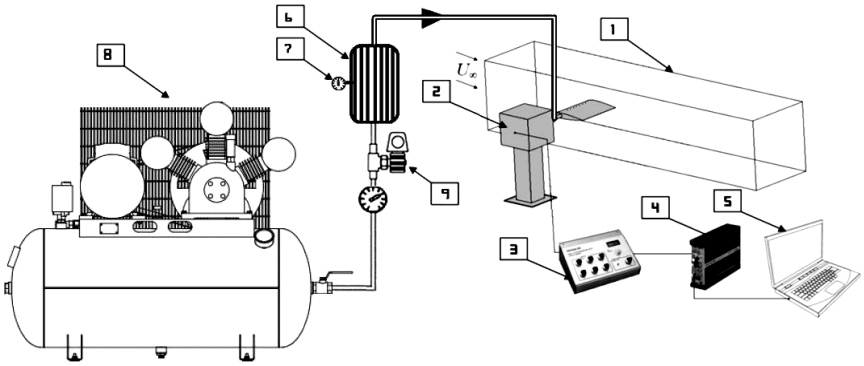

Figure 1. Sketch showing the wind tunnel and blowing device (1: Test tunnel, 2: Aerodynamic balance, 3: Stress indicator, 4: Converter, 5: Acquisition and processing of data on computer, 6: Stilling chamber, 7: Pressure gauge , 8: Air compressor, 9: Valve)

Wind Tunnel And Acquisition Chain

NACA 4412 Airfoil

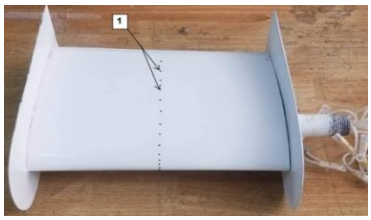

Figure 2. NACA 4412 airfoil (1: static pressure taps).

The aerodynamic profile used in the experiments is a cambered NACA 4412 airfoil with a chord length of 150mm, a span of 200mm, a maximum camber of 4% of the chord, and a maximum thickness of 12%, as

indicated in its designation. Two endplates were used to minimize the 3D end effects on the airfoil. They were constructed from steel sheets and measured 200mm × 50mm, with a radius of 25mm. These dimensions were chosen in consideration of the wind tunnel test section dimensions to minimize aerodynamic blockage effects. The airfoil is equipped with fourteen pressure taps arranged along its mid-chord line (Figure 2).

NACA 4412 Wing

The model created is a wing with a 5° sweep angle, built using a NACA 4412 airfoil, featuring a mid-chord length of 140 mm and a span of 200 mm (Figure 3). It is equipped with 10 micro-holes of 0.6 mm diameter evenly arranged at 10% of the leading edge. The micro-holes, employed for blowing, are oriented at a 45° angle relative to the wing's chord (Figure 4).

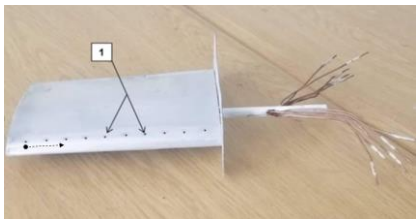

Figure 3. NACA 4412 wing (1: blowing holes).
The numbering direction of the blowing orifices is indicated by the dashed arrow (from 1 to 10).

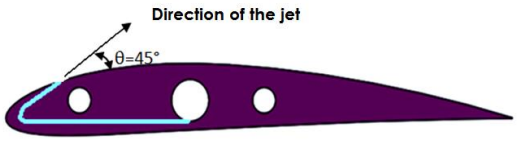

Figure 4. Sectional view showing the position of the blowing orifices on the model.
The arrow indicates the jet direction as well as the tilting angle θ of the blowing nozzles.

Blowing Device

To achieve flow control around the NACA 4412 wing, the blowing device primarily consists of an air compressor, a stilling chamber, and a flow control valve. The Schneider-type compressor compresses air, achieving a maximum relative pressure of 16 bar. Compressed air flows through a valve used to regulate pressure in the generating state, then it is directed into the stilling chamber designed to minimize turbulence caused by the compressor. It is then conveyed to a ramp constructed from a copper tube with a diameter D=14mm, onto which capillary tubes are implanted, each having an outlet section with a diameter d=0.6mm. The ten capillary tubes are connected to the blowing orifices of the wing.

Our blowing configuration can be likened to a convergent nozzle, where the nozzle throat corresponds to the cylindrical opening of the capillary tubes used for blowing. To better characterize the flow at the blowing orifices, it is essential to establish a relationship between the air pressures measured in the generating state and in the immediate vicinity of the micro-orifices, and the ejected air flow. The latter is determined by the following equation:

$$Q_j = S_j \sqrt{\frac{2k}{(k-1)} \frac{P_t}{\nu_t} \left(\left(\frac{P}{P_t} \right)^{2/k} - \left(\frac{P}{P_t} \right)^{(k+1)/k} \right)} \tag{1}$$

With: k: Adiabatic constant, P_t: Total pressure in the generating state, ν_t: Specific volume at the generating state. The jet velocity V_j is determined from the flow rate using the following expression:

$$V_j = \frac{\nu Q_j}{S_j} \tag{2}$$

Blowing through micro-jets is performed in eight distinct modes based on the number of open orifices and the blowing pressure in the generating state. Table 1 illustrates the eight jet modes.

Table 1. Various blowing modes tested in a wind tunnel. With (1: opened hole and 0: closed hole).

	Hole number									
Mode	**1**	**2**	**3**	**4**	**5**	**6**	**7**	**8**	**9**	**10**
a	*1*	*1*	*1*	*1*	*1*	*1*	*1*	*1*	*1*	*1*
b	*1*	*1*	*1*	*1*	*1*	*0*	*0*	*0*	*0*	*0*
c	*0*	*0*	*0*	*0*	*0*	*1*	*1*	*1*	*1*	*1*
d	*1*	*1*	*0*	*0*	*1*	*1*	*0*	*0*	*1*	*1*
e	*0*	*0*	*1*	*1*	*0*	*0*	*1*	*1*	*0*	*0*
f	*1*	*0*	*1*	*0*	*1*	*0*	*1*	*0*	*1*	*0*
g	*0*	*1*	*0*	*1*	*0*	*1*	*0*	*1*	*0*	*1*
h	*0*	*1*	*1*	*1*	*0*	*1*	*1*	*1*	*1*	*0*

Aerodynamic Coefficients

The lift and drag coefficients are measured using the aerodynamic balance connected to the airfoil. These aerodynamic coefficients are commonly defined as follows:

$$C_{D,L} = \frac{F_{x,y}}{\frac{1}{2}\rho U_{\infty}^{2} S_{\infty}} \tag{3}$$

With: $F_{x,y}$: Aerodynamic lift and drag forces, ρ : Air density, S_{∞} : Wing area, U_{∞}: Free-stream velocity.

Results and Discussion

In this section, the results of the experiments conducted with the two models (airfoil and NACA 4412 wing) are presented. Measurements were taken over an angle of attack range from 0° to 25°, for two flow Reynolds numbers: Re=1.6×10^5 and Re=2.5×10^5.

Uncontrolled Flow

Aerodynamic Forces in the Case of the Airfoil and NACA 4412 Wing

Measurements of aerodynamic forces are conducted for various attack angles using an aerodynamic balance (see Figure 1). The curves of lift and drag coefficients as a function of attack angle (uncorrected for the blockage effect) are depicted in Figures 5.a and 5.b for two Reynolds numbers.

In the case of the NACA 4412 airfoil, it can be observed from these figures that the stall angles are 16° and 18°, respectively, for Re=1.6×10^5 and Re=2.5×10^5. Beyond these angles, there is a noticeable increase in drag values due to aerodynamic stall. As for the flow around the 5° sweep wing, both lift and drag forces are lower compared to the airfoil case. The lift curves exhibit a non-linear trend at low attack angles, indicating the presence of the wingtip vortex that disrupts the pressure distribution around the wing. Stall occurs in this case at 17° and 18°, respectively, for Re=1.6×10^5 and Re=2.5×10^5.

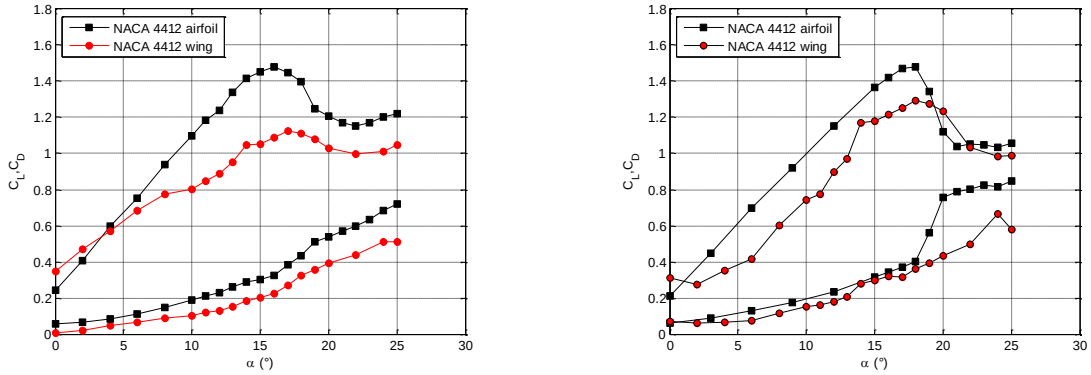

a) Re=1.6×10^5. b) Re=2.5× 10^5.

Figure 5. Evolution of lift and drag coefficients as a function of attack angle, uncontrolled case.

Pressure Field around the NACA 4412 Airfoil

The flow properties around the uncontrolled NACA 4412 airfoil are initially studied, and the corresponding distributions of the static pressure coefficient are determined. Figures 6.a-b show the distributions of the static pressure coefficient around the NACA 4412 airfoil for angles of attack ranging from [0°-25°] and two flow Reynolds numbers [1.6×10^5; 2.5×10^5]. Since the NACA 4412 is a cambered airfoil, at zero angle of attack, the static pressure on the airfoil is asymmetric, resulting in the existence of lift force (Figures 45.a-b). There are regions of accelerated flow on the airfoil that reach the highest depressions, corresponding to the maximum thickness of the airfoil at zero incidence. The maximum pressure occurs at the stagnation point where the velocity is zero.

As the airfoil attack angle is increased to around 18°, the adverse pressure gradient imposed on the boundary layers becomes so significant that flow separation occurs. A recirculation flow region over almost the entire upper surface of the airfoil is formed. Consequently, lift decreases significantly, and drag increases sharply. For a further increase in the attack angle, the stagnation point moves significantly toward the trailing edge on the lower surface. The recirculation flow region becomes dominant, covering the entire upper surface; the air flow is completely separated from the airfoil surface. This leads to a further reduction in lift force and a substantial increase in drag force. This situation is characterized by the formation of an almost constant C_P plateau (see Figure 5, α=25°).

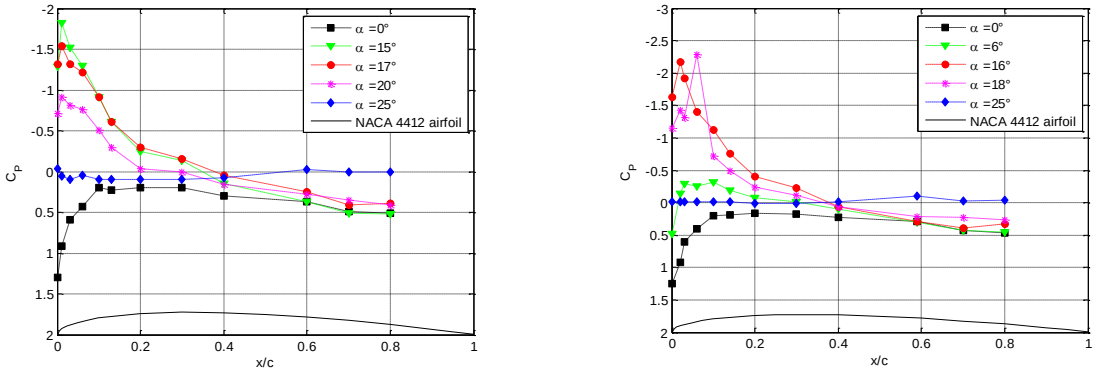

a) Re=1.6×10^5. b) Re=2.5× 10^5.

Figure 6. Evolution of the pressure coefficient at various attack angles of the airfoil, without control.

Controlled Flow

The action of the micro-jet on a wing allows for a remarkable influence on aerodynamic coefficients. However, to optimize this type of blowing system, it is necessary to study the influence of certain parameters, either adjustable by the user or imposed by the technology of the blowing device used. Indeed, the influence of varying the blowing rate, wing incidences, and the free-stream velocity upstream has been analyzed during the test series conducted in the laboratory. Other geometric parameters such as diameter, spacing, position relative

to the chord of the holes, and their tilt angle are kept constant. However, the control efficiency may change by varying these geometric parameters, making the optimization study of control efficiency appear somewhat simplified.

Aerodynamic Forces of the Controlled Boundary Layer by Blowing in the Case of the NACA 4412 Wing

a. Effect of tangential blowing on control efficiency

The control is achieved through continuous jets via a series of 0.6 mm diameter orifices located on the upper surface of the NACA 4412 wing (Figure 3). The micro-orifices are positioned at 10% from the leading edge. Figure 7, presented as a histogram, illustrates the lift gains obtained for all blowing modes (Table 2) tested in the wind tunnel at a Reynolds number of 1.6×10^5. It is evident from these results that a more significant lift improvement is recorded for mode (a) and at a pressure Pr=2.0 bar, corresponding to full blowing.

Considering the results in Figure 7, it is apparent that for mode (b), no lift gain is recorded. This can be explained by the fact that the position of the blowing orifices (blowing on the left half of the wing) for this mode is not conducive to boundary layer reattachment to the wall. Instead, it acts on reducing the cross-sectional area of the wake, directly influencing induced drag (Refer to the following section), which is a consequence of limiting the wing's aspect ratio (transition from two-dimensional to three-dimensional aerodynamics).

Delays in stall, ranging from 1 to 2 degrees, are also observed in some blowing modes such as mode (b), (e), (f), and (g). Moreover, blowing control on this type of wing did not result in any reduction in drag. On the contrary, parasitic drag is observed for almost all blowing modes, except for mode (b), where a maximum drag reduction of 70% was measured at an incidence of 10 degrees.

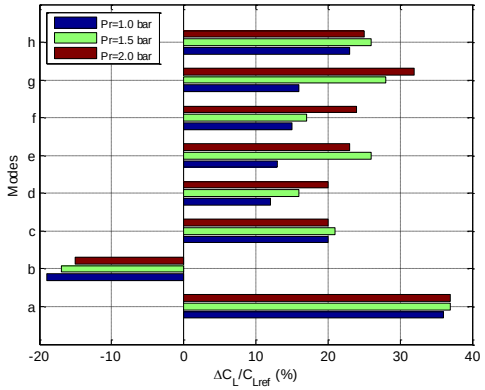

Figure 7. Lift gains obtained for different blowing modes, Re=1.6 × 10^5.

b. Effect of Blowing Rate

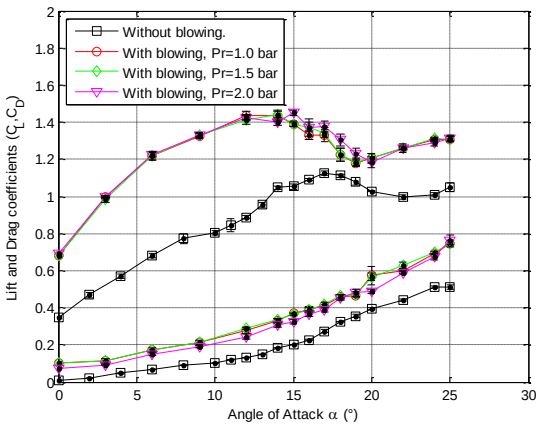

Figure 8. Evolution of the lift and drag coefficients as a function of attack angle, with and without control. Re=1.6 × 10^5, mode (a).

Significant improvements in the lift coefficient and a delay in stall are observed with control (Figure 7). The increase in the lift coefficient is closely related to the increase in the blowing rate. In the absence of blowing, the profile stalls at 16° for Re=1.6×10^5. The effect of control begins even at low angles of attack; a gradual increase in lift is observed, noticeable for all angles of attack before stall. Comparing the control curves, it is evident that they are relatively close for all attack angles ; there is a saturation of the lift coefficient, and the control effect is limited by the sonic blockage phenomenon at the blowing holes.

It is also interesting to analyze the effect of control on the drag coefficient. The trends of the C_D coefficient shown in Figure 8 indicate that the drag of the controlled case evolves roughly in the same manner, exhibiting a parasitic increase.

c. Effect of Reynolds number on aerodynamic coefficients

Figures 8 and 9 show the overlay of lift and drag coefficients curves for the reference case and with control using the micro-holes. For both Reynolds numbers studied, an improvement in lift is observed. At a Reynolds number of 2.5×10^5, the control effect on the lift coefficient is slightly less effective than in the case with Re=1.6×10^5. Specifically, a 37% lift gain is recorded for flow at 1.6×10^5, and only a 4% relative lift increase is observed for the second case (Re=2.5×10^5) compared to C_{Lmax}, with a 2° delay in stall. The analysis of drag reveals a greater production of parasitic drag in flows with low Reynolds numbers at high angles of attack.

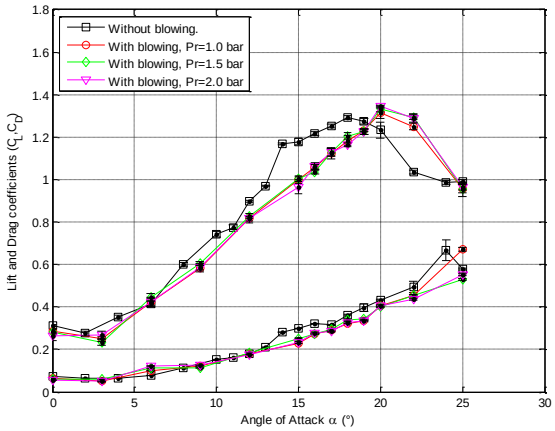

Figure 9. Evolution of the lift and drag coefficients as a function of attack angle, with and without control. Re=2.5×10^5, mode (a).

Pressure Coefficient around the NACA 4412 Wing with and without Flow Control

The results depicted in the figures below are analyzed based on the averaged mappings of static pressure loss Cp. Energy losses associated with pressure drag significantly contribute to the development of total aerodynamic drag. Pressure measurements are conducted using a wake rake positioned 250 mm downstream from the wing's leading edge. This rake consists of fifteen capillary tubes spaced 10 mm apart and oriented in the flow direction. The wake is scanned with a regular 10 mm step along the y-axis, forming a measurement plane of 15×12 cm². Total pressures are measured using a differential manometer. The evolving pressure shown therein clearly indicates the wake's depression.

Vortex shedding occurs wherever a lifting surface ends in a fluid. The flow around the NACA 4412 wing generates lift by producing low static pressures above the wing and comparatively higher pressures below. This pressure difference between the upper and lower wing surfaces accelerates the fluid around the wingtip, creating a marginal vortex. This is clearly discernible in the Cp iso-value maps for the uncontrolled case (Figure 10).

When blowing occurs near the wing surface, despite the significant improvements in lift recorded, the previously observed drag measurement indicates a tendency to increase. This is supported by the calculation of the average Cp value for the uncontrolled case (Cp_{moy}=0.59, See Figure 10) and the controlled case (Cp_{moy}=0.63, See Figure 11). The increase in drag is directly related to the locally created depression by blowing at the upper surface, which remains insufficient to reattach the fluid streamlines on the wing.

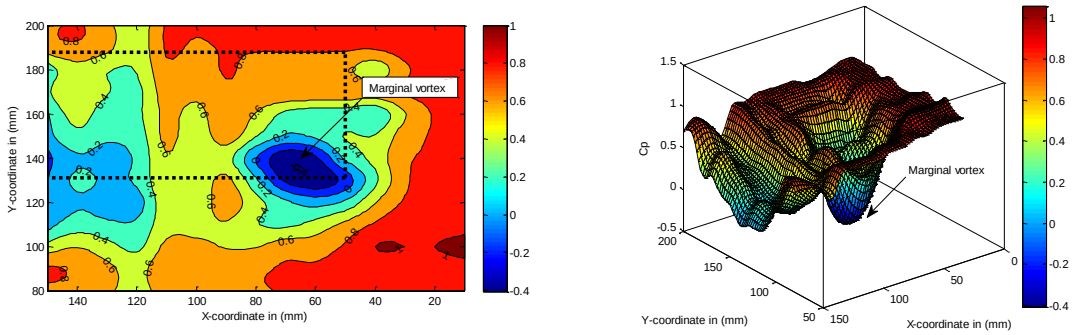

a) Isovalue contours of the pressure coefficient. b) Three-dimensional pressure coefficient.

Figure 10. Static pressure coefficient recorded at Z/c=1.67, Re=1.6×10^5, α=15°. The dashed lines represent the wing contour.

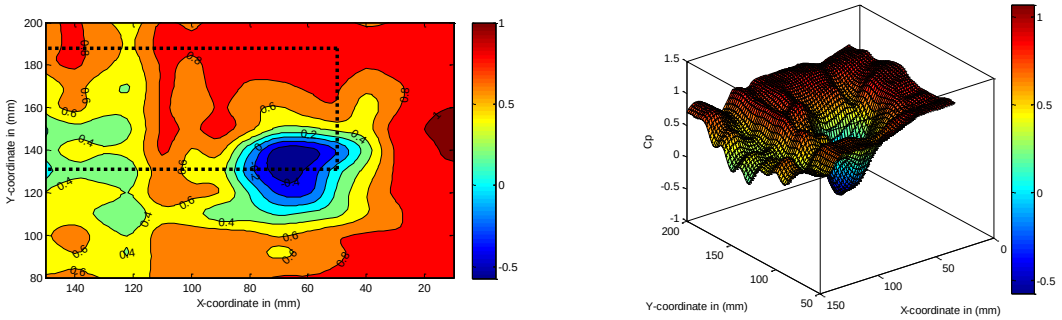

a) Isovalue contours of the pressure coefficient. b) Three-dimensional pressure coefficient.

Figure 11. Static pressure coefficient recorded at Z/c=1.67, Re=1.6×10^5, α=15°, mode (a), Pr=2.0 bar. The dashed lines represent the wing contour.

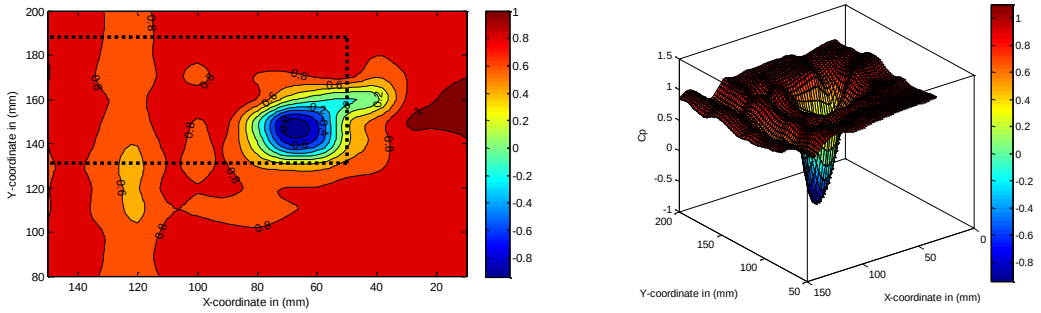

a) Isovalue contours of the pressure coefficient. b) Three-dimensional pressure coefficient.

Figure 12. Static pressure coefficient recorded at Z/c=1.67, Re=1.6×10^5, α=17°, without control. The dashed lines represent the wing contour.

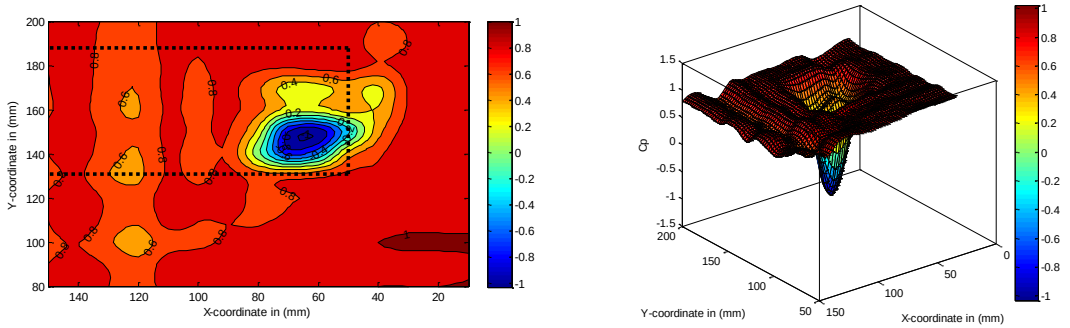

a) Isovalue contours of the pressure coefficient. b) Three-dimensional pressure coefficient.

Figure 13. Static pressure coefficient recorded at Z/c=1.67, Re=2.5×10^5, α=17°, mode (a), Pr=2.0 bar, with control. The dashed lines represent the wing contour.

Similarly, for flow at a high Reynolds number ($Re=2.5\times10^5$), an increase in the average Cp value from the uncontrolled case (Cp=0.77, see Figure 12) to the controlled case (Cp=0.79, see Figure 13) is observed. However, the intensity of the vortex is much more pronounced in this case compared to the results at $Re=1.6\times10^5$. The performance of the control necessarily degrades in 3D (in the case of a wing) due to the presence of highly energetic longitudinal vortex structures. Nevertheless, the results presented here still serve as an interesting foundation for the exploration of three-dimensional solutions. In this regard, the topology of the wake flow must be analyzed to identify the control mechanisms and the origins of drag reduction.

Conclusion

The results of this present study emphasize the importance of blowing through the micro-orifices. In the case of the NACA 4412 wing, the effects of controlling the blowing rate at Reynolds numbers ranging from (1.6×10^5 – 2.5×10^5) and different angles of attack are evaluated. When the stagnation pressure is varied and analyzed over the range of (1.0 – 2.0 bar), the following results were obtained:

- Although the steady blowing was only performed at 10% of the chord, the results indicate that an increase in blowing pressure enhances the aerodynamic coefficients. Indeed, a very noticeable increase in maximum lift of about 37% is achieved when Pt=2.0 bar, and at a Reynolds number equal to 1.6×10^5. These lift gains depend on the Reynolds number of the flow. Additionally, a significant reduction in drag of approximately 20% is observed for a specific blowing mode (b).

- A delay in stall of about two degrees is achieved.

- To achieve a real improvement in aerodynamic performance, it appears necessary to apply an optimization approach to the position of the micro-holes, the inclination angle, as well as their diameter. These parameters influence the coherent flow structures and can delay or even eliminate boundary layer separation.

Scientific Ethics Declaration

The authors declare that the scientific ethical and legal responsibility of this article published in EPSTEM Journal belongs to the authors.

Acknowledgements or Notes

* This article was presented as a poster presentation at the International Conference on Technology, Engineering and Science (www.icontes.net) held in Antalya/Turkey on November 14-17, 2024.

References

Bourgois, S. (2006). *Etude Expérimentale du Décollement Sur profils d'aile : Analyse et contrôle* (Doctoral dissertation). Université de Poitiers. Retrieved from https://tel.archives-ouvertes.fr/tel-00308715

Chen, Y., Avital, E., Willams, J., Santra, S., & Seifert, A. (2024). Effects of leading-edge blowing control and reduced frequency on airfoil aerodynamic performances. *Journal of Fluids Engineering*, *146*(10),1-56.

Coustols, E., Stumpf, E., Jacquin, L., Moens, F., Vollmers, H., & Gerz, T. (2003). "Minimised wake": A collaborative research programme on aircraft wake vortices. *41st Aerospace Sciences Meeting and Exhibit*.

Favier, J., Bourgois, S., Sommier, E., Tensi, J., & Kourta, A. (2005). Contrôle fluidique du décollement sur un profil d'aile. *In 17ème Congrès Français de Mécanique*.

Gad-el-Hak, M. (2001). Flow control. The future. *Journal of Aircraft*, *38*(3), 402–418.

Haverkamp, S., Neuwerth, G., & Jacob, D. (2005). Active and passive vortex wake mitigation using control surfaces. *Aerospace Science and Technology*, *9*(1), 5-18.

Jupp, J. (2001). Wing aerodynamics and the science of compromise. *The Aeronautical Journal*, *105*(1053*)*, 633–641.

Kroo, I. (2001). Drag due to lift: concepts for prediction and reduction. *Annual Rev: Fluid Mechanics*, *33*(1), 587–617.

Manolesos, M., & Voutsinas, S. G. (2016). Experimental study of drag-reduction devices on a flatback airfoil. *AIAA Journal*, *54*(11), 3382-3396.

Roumeas, M. (2006). *Contribution à l'analyse et au contrôle des sillages de corps épais par aspiration ou soufflage continu* (Doctoral dissertation). Institut National Polytechnique de Toulouse. Retrieved from https://oatao.univ-toulouse.fr/7493/1/roumeas.pdf

Satar, M. H. A., Razak, N. A., Abdullah, M. S., & Ismal, F. (2024). A comprehensive comparison of passive flow controls on the wind turbine blade lift and drag performances. A CFD approach. *European Journal of Mechanics-B/Fluids, 108*, 119-133.

Schlichting, Hermann. (1979). *Boundary layer theory*. New York. NY: McGraw-Hill.

Sloof, J., de Wolf, W., van der Wal, H., & Masel&, J. (2002). Aerodynamic and aero-acoustic effects of flap tip fences. *40th AIAA Aerospace Sciences Meeting and Exhibit.*

Author Information

Hocine Tebbiche
Mouloud MAMMERI University of Tizi-Ouzou
15000, Tizi-Ouzou, Algeria
Contact e-mail: *hocine.tebbiche@ummto.dz*

Mohammed Saîd Boutoudj
Mouloud MAMMERI University of Tizi-Ouzou
15000, Tizi-Ouzou, Algeria

To cite this article:

Tebbiche, H. & Boutoudj, M.S. (2024). Micro-jet control of flow in NACA 4412 wing. *The Eurasia Proceedings of Science, Technology, Engineering & Mathematics (EPSTEM), 32*, 106-115.